MedCrave
Step into the World of Research
International Journal of Petrochemical Science & Engineering

Research Article
Open Access
CrossMark

# Adsorption isotherm, kinetic, thermodynamic and breakthrough curve models of $H_2S$ removal using $CeO_2$/NaOH/PSAC

## Abstract

Dynamic adsorption is not suitable to be used to find the adsorption isotherm for $H_2S$ removal. It was because the conventional experimental method used grain adsorption for the isotherm calculation. In order to achieve grain adsorption using the fixed bed adsorption test rig, the amount of adsorbent was minimized to create a similar operation compare to grain adsorption, allowing the proper calculation of isotherm parameters. Data analysis showed that Freundlich sorption isotherm can best described the sorption behavior. Thermodynamic study showed that enthalpy change (ΔH) and entropy change (ΔS) were calculated to be -6.0 kJ/mol and 25.7 J/mol.K. The sorption was pseudo-second order with activation energy 11.7 kJ/mol and rate constant was between 2.387–4.066 X $10^{-6}$ g/mg.min for 30-70˚C. Breakthrough curve was fitted best by using breakthrough model developed by.[1]

**Keywords:** adsorption isotherm, kinetic, thermodynamic, breakthrough curve model, hydrogen sulfide, activated carbon

Volume 1 Issue 2 - 2016

Lee Chung Lau,[1] NorhusnaMohamadNor,[2] KeatTeongLee,[3] Abdul Rahman Mohamed[3]
[1]Department of Petrochemical Engineering, Universiti Tunku Abdul Rahman, Malaysia
[2]Faculty of Chemical Engineering, Universiti Teknologi Mara, Malaysia
[3]School of Chemical Engineering, Universiti Sains Malaysia, Malaysia

**Correspondence:** Lee Chung Lau, Department of Petrochemical Engineering, Universiti Tunku Abdul Rahman, Malaysia, Tel +605-4688888, Fax +6054667449, Email laulc@utar.edu.my

**Received:** August 08, 2016 | **Published:** October 20, 2016

## Introduction

Adsorption isotherm describes the equilibrium relationship of $H_2S$ distribution in the bulk gas stream and on the surface of an adsorbent.[2] This equilibrium data is crucial and required in the process design of the adsorption systems.[3] There are various models developed such as Langmuir, Freundlich, Temkin and Dubinin-Radushkevich isotherms. These isotherms generally are empirical models and used linear regression to fit the experimental data. Dynamic and static adsorption was performed by.[4] They reported that dynamic and static adsorption of $H_2S$ will result differently. For dynamic adsorption, it is not suitable used for finding adsorption isotherm. Equilibrium study needs to use static adsorption to find data able to fit with adsorption isotherms. During dynamic adsorption, external $H_2S$ concentration was constant because it was supplied continuously. Therefore, the driving force for $H_2S$ was not identical with grain adsorption. In addition, if a lot of adsorbent was used for dynamic adsorption, the adsorption capacity will increase with lower $H_2S$ concentration. For grain adsorption, adsorption capacity will decrease with lower $H_2S$ concentration.

Langmuir model was developed to describe the adsorption of gases onto adsorbents with the assumption that the gases are adsorbed in the monolayer pattern.[5–8] In addition, there is finite number of adsorption sites on the solids that are same with identical potential energy. In another word, homogeneously structured adsorbent is assumed in developing the Langmuir equation.[9] In the context of adsorption on micro porous adsorbents, the idealized monolayer adsorption of this model is not applicable, even though the characteristic form of Langmuir model (Type I) is found for the micro porous adsorbents. The major reason for this claim is the characteristic form found using the micro porous adsorbent is due to the micro pore volume-filling process, but not the monolayer surface coverage as described by Langmuir model.[10]

On the other hand, Freundlich model was one of the earliest developed models to describe the adsorption process. It is empirical and used in the non–ideal adsorption process. Therefore, it is considered as a model involving the measure of heterogeneous adsorption.[9,11–13] If the heterogeneity factor in the equation is larger than one, the adsorbent surface is becoming more heterogeneous. The weakness of this isotherm is the under prediction and over prediction of the adsorption capacity at the intermediate and high equilibrium, respectively.[2]

Features from Langmuir and Freundlich isotherm can be incorporated into a new isotherm named Redlich-Peterson isotherm. It contains three parameters and can be solved using trial and error optimization method. By using computer software such as Microsoft Excel, the coefficient of determination, $R^2$ can be determined easily. The values of three parameters that result highest $R^2$ value is considered as the solution of the Redlich-Peterson isotherm.[14] Dubinin-Radushkevich isotherm is developed based on the volume-filling theory of micro pores and combination of Polanyi's adsorption potential theory.[15,16] Energy of adsorption can be derived from this isotherm and subsequently it can be linked with the average micro pore width.[10] Temkin model, on the other hand, was derived from the assumption that the heat of adsorption is decreasing linearly rather than logarithmically.[4,14,17]

Dynamic adsorption is not suitable to be used to find the adsorption isotherm for $H_2S$ removal. From the result of dynamic adsorption reported elsewhere, it was found that higher $H_2S$ concentration did not necessarily result higher adsorption capacity. Therefore, the isotherm parameters obtained in this case cannot be explained by conventional adsorption isotherm theory. In fact, it was because the conventional experimental method used grain adsorption for the isotherm calculation. In order to achieve grain adsorption using the fixed bed adsorption test rig, the amount of adsorbent was minimized to an extent that $H_2S$ at outlet stream was detected within a minute of operation. This created a similar operation compare to grain adsorption, allowing the proper calculation of isotherm parameters.

Adsorption kinetic relates the rate of adsorption of specific amount of adsorb ate onto the surface or porous structure of a unit amount of adsorbent. In an adsorption process, it is considered as reversible process as desorption could occur also, but not in the initial stage. In the later stage of adsorption process, desorption will become more significant and active because sufficient amount of adsorb ate has been adsorbed and create higher driving force for desorption to occur.[14] Due to the time dependent nature of adsorption process, kinetic study is important so that the rate of adsorption can be determined, subsequently plays an important role in the process design of the adsorption system.[3]

Several thermodynamic parameters can be determined from the adsorption thermodynamics study. These parameters provide information regarding the behavior of adsorption process. Among these, enthalpy change, Gibbs free energy and entropy are the most popular thermodynamic parameters studied. These parameters have their own physical meanings. Enthalpy change is the heat adsorbed or released during the reaction; Gibbs free energy can be regarded as the minimum isothermal work for the adsorbent to reach a certain energy level; and adsorption entropy provides information of the randomness and the packing manner of the adsorbed species.[9]

Enthalpy change of $H_2S$ adsorption on the activated carbon is generally negative (exothermic) and can be categorized as physical or chemical adsorption. The difference between these two types of adsorption is their range of enthalpy change or more specifically named as heat of adsorption. Heat of physical adsorption is about 8-25 kJ/mol. This energy is released during the change of intermolecular force between the adsorb ate and the adsorbent. Chemical adsorption on the other hand, change the molecular structure of the adsorb ate to form new bonding with adsorbent such as ionic, covalent and hydrogen bond. The energy released from the new bonding generally ranges from 40-200 kJ/mol. In an adsorption process, it is important to quantify the heat of adsorption to ensure the operation is safe. If the heat of adsorption is accumulated in the system, excess heating of the work place or explosion could bring hazard. Apart from that, the released heat will alter the sorbent temperature and subsequently affect the operation because there are changes in mass transfer and adsorption process.[18] It is interesting to note that even though adsorption process is normally regarded as exothermic process;[18] also reported endothermic adsorption in the low temperature region (20-60˚C). The adsorption heat was changed to exothermic in the higher temperature region (60-150˚C). They explained that in different temperature region, the significant process that contributes to the adsorption heat was different. In low temperature region, the adsorption heat was affected by the amount of adsorbed water on the surface and in high temperature region, the chemical interaction had higher influence over the heat of adsorption.[18]

Breakthrough curve carries the information about the dynamic behavior of the effluent concentration in time and therefore crucial for the adsorption column design.[19] In order to predict the dynamic behavior of an adsorption column, mathematical models are needed. These models are crucial for the sizing and optimization of the actual industrial process developed from laboratory data. Various mathematical empirical models have been developed to predict the dynamic breakthrough curve behavior of the adsorption column.[20] Among these, several models discussed were Bohart-Adams, Wolborska, Thomas and Yoon-Nelson models. Bohart-Adams model was derived by assuming that the rate of adsorption can be related to the residual adsorption capacity of the adsorbent and the concentration of pollutant. This model was used to describe the initial part of the breakthrough curve.[21,22] For Wolborska model, derivation was assumed using low concentration range of the breakthrough curves. The diffusion mechanism was described using general equation of mass transfer.[23,24] On the other hand, Thomas model, was applied to a constant flow rate system with no axial dispersion. It also possesses behavior similar to Langmuir isotherm and second order reaction kinetics.[19] Last but not least, Yoon-Nelson model was a relative simple model derived for a single component system only.[22,24]

In the breakthrough curve modeling, rigorous model that includes axial dispersion, external film resistance and intraparticle diffusion is complex mathematically and difficult to be used because some parameters employed are unavailable.[1] Therefore, simple modeling approach by using approximation of linear driving force model or assumption of local equilibrium which avoids the difficulty in solving partial differential equation and considering the kinetics of adsorption, respectively.[1]

## Experimental

### a. Chemicals

The palm shell activated carbon (PSAC) used in this study was steam activated and purchased from Victory Element SdnBhd, Malaysia. Upon receiving, the PSAC was sieved to 1-2 mm and dried at 80˚C in an oven. In the PSAC impregnation, extra pure (98.5%) cerium (III) nitrate hexahydrate ($Ce(NO_3)_3.6H_2O$) and analytical reagent grade sodium hydroxide (99% NaOH) in pellet form supplied by Merck SdnBhd were used. Purified nitrogen (99.99% $N_2$) was used in the calcination of the impregnated activated carbon. In $H_2S$ adsorption test, three types of gases (99.99% $CH_4$, 99.99% $CO_2$ and 1% $H_2S$, balance $CH_4$) in cylinders supplied by Wellgas SdnBhd, Malaysia were used to simulate the industrial biogas.

### b. PSAC impregnation

Cerium nitrate solution at 5 wt% cerium corresponding to PSAC amount was first added to 2.50 g PSAC in a conical flask. Then, sodium hydroxide at 1.0 M was added to the flask slowly. Subsequently, the mixture was shacked in a water bath shaker at room temperature for 1.5 h impregnation time. After that, the impregnated activated carbon will be filtered and dried in an oven at 80˚C. The dried impregnated activated carbon was then subjected to 400˚C calcination temperature and three hours calcination time under the flow of $N_2$ at 50 mL/min.

### c. Adsorption test

$H_2S$ adsorption test was carried out using a packed bed reactor test rig as shown in Figure 1. The composition of simulated biogas was adjusted by controlling the flow rate of gases using Aalborg AFC26 mass flow controllers. $CO_2$ and $CH_4$ were passed through a humidification system at room temperature to provide moisture to the biogas inlet stream at about 25% relative humidity. $H_2S/CH_4$ was not passed through the humidification system because $H_2S$ is soluble in water. The path of the biogas after the humidification system to the reactor is insulated to avoid condensation of moisture. The diameter of the stainless steel tubular reactor used is half inch. The flow rate of the biogas was fixed at 500 mL/min with $CO_2$, $H_2S$ and $CH_4$ in specific concentration. The amount of adsorbent was 0.1g for isotherm study; 1.0g for kinetic and thermodynamic study. The adsorbent was placed in the middle of the tubular reactor and supported with approximately

0.05g glass wool. Adsorption temperature (30-70˚C) was controlled using a Linberg/Blue M tube furnace. Concentration of $H_2S$ at the outlet stream was analyzed using an IMR 6000 gas analyzer via electrochemical sensor calibrated for 0-5000 ppm $H_2S$. The workspace of the test rig was ventilated as a safety procedure just in case there is a leakage of hazardous $H_2S$.

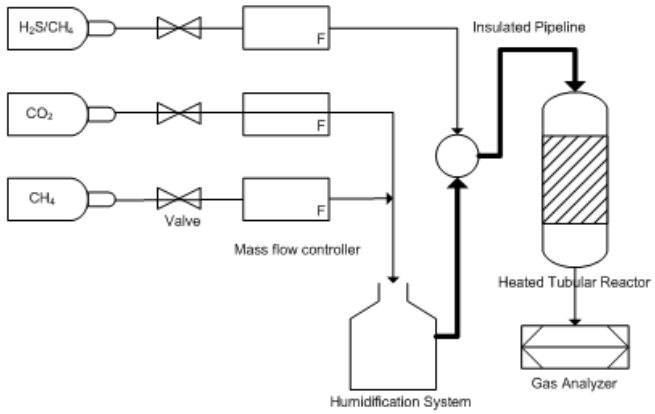


**Figure 1** $H_2S$ adsorption test rig.

## Results and discussion

### a. Adsorption isotherm

The breakthrough curves of $H_2S$ removal using 0.1g adsorbent for different $H_2S$ concentration was shown in Figure 2. For all studies, $H_2S$ was detected at outlet stream in the first minute of operation. Then, the $H_2S$ concentration gradually increased until it was equal with the inlet concentration. The adsorption capacity at different $H_2S$ concentration was recorded in mg/g and the $H_2S$ concentration in ppm was converted to mg/L, for the ease of calculation. The calculations for the adsorption isotherms were tabulated in Table 1. Several adsorption isotherm were used to fit the experimental data using linear regression method. Among these, Langmuirand temkin did not fit well with the experimental data. On the other hand, Freundlich, Dubinin-Radushkevich and Redlich-Peterson were able to fit with experimental data to give a $R^2$ value above 0.95.

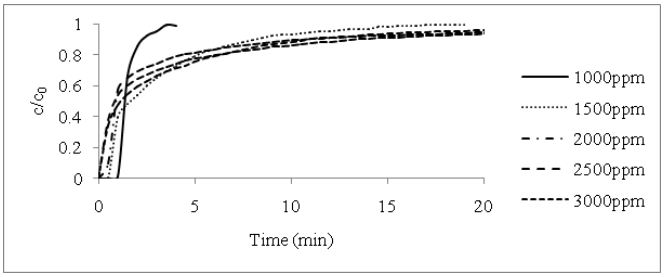


**Figure 2** Breakthrough curve at different $H_2S$ concentration using 0.1g adsorbent, for adsorption isotherm study.

Langmuir isotherm describes a monolayer adsorption on the adsorbent surface. The model can be expressed by the equation below:

$$Q_e = \frac{K_L Q_m C_e}{1 + K_L C_e} \quad \text{Eq. (1)}$$

Eq. (1) can be rearranged to the linearized form:

$$\frac{Ce}{Q_e} = \frac{1}{Q_m} Ce + \frac{1}{K_L Q_m} \quad \text{Eq. (2)}$$

where $K_L$ and $Q_m$ are the Langmuir isotherm constant related to the binding energy and monolayer adsorption capacity, respectively.

**Table 1** Adsorption isotherms calculations

| S.No | $C_e$ | $Q_e$ | $C_e/Q_e$ | $lnC_e$ | $lnQ_e$ | $(ln(1+1/C_e))2$ |
|---|---|---|---|---|---|---|
| 1 | 4.11 | 116.18 | 0.035 | 1.41 | 4.76 | 0.047 |
| 2 | 3.43 | 84.42 | 0.041 | 1.23 | 4.44 | 0.066 |
| 3 | 2.74 | 43.76 | 0.063 | 1.01 | 3.78 | 0.097 |
| 4 | 2.06 | 30.38 | 0.068 | 0.72 | 3.41 | 0.157 |
| 5 | 1.37 | 8.9 | 0.154 | 0.32 | 2.19 | 0.3 |

The correlation of Langmuir isotherm was presented in Figure 3. It was clearly seen that this isotherm did not fit the experimental data well, with a correlation coefficient, $R^2$ value of only 0.7631. Langmuir isotherm had been successfully applied in much pollutant adsorption process but it is more common for the adsorption of a pollutant from a liquid solution.[25] Therefore, it is reasonable to find Langmuir isotherm not suitable to fit these experimental data obtained via adsorption from a gaseous stream.

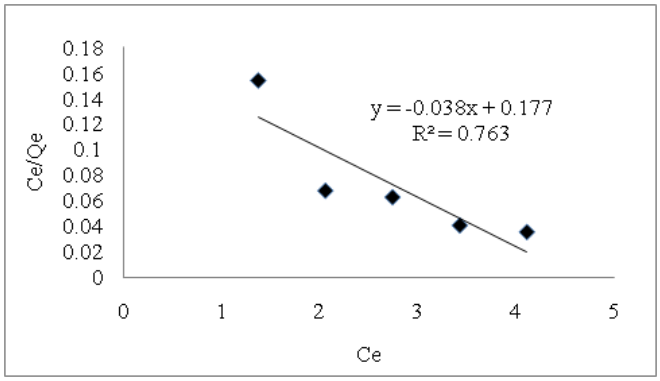


**Figure 3** Langmuir adsorption isotherm.

Temkin isotherm was derived by assuming that the heat of adsorption reduces in a linear way, rather than a logarithmic way. In addition, it is applicable to chemical adsorption only, with uniformed binding energy.[26] Temkin isotherm is expressed in the following equation:

$$Q_e = \frac{R_T}{b_T} \ln\left(A_T C_e\right) \quad \text{Eq. (3)}$$

Eq. (3) can be rearranged to the linearized form:

$$n\, Q_e = \frac{R_T}{b_T} lnC_e + \frac{R_T}{b_T} lnA_T \quad \text{Eq. (4)}$$

Where $b_T$ and $A_T$ are Temkin constants related to the heat of adsorption.

Figure 4 denoted the Temkin isotherm in the linearized form. The

correlation coefficient was only 0.8993, implied that Temkin isotherm did not well describe the experimental data. This could mean that the $H_2S$ adsorption using $CeO_2$/NaOH/PSAC adsorbent was not really a chemical adsorption process.

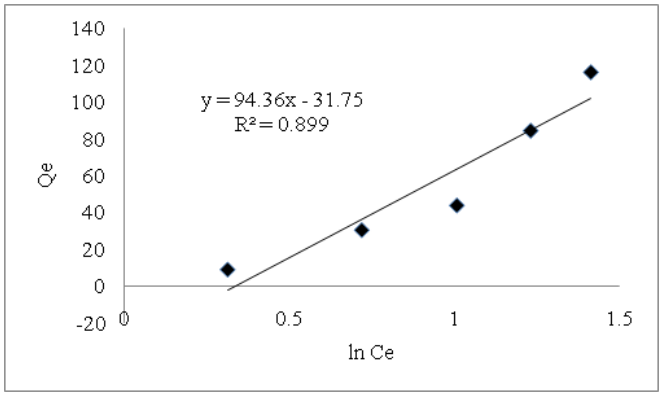


**Figure 4** Temkin adsorption isotherm.

Freundlich isotherm was the earliest proposed adsorption isotherm in 1906. It is an empirical model to predict multilayer adsorption on heterogeneous surface. However, it does not reduce to Henry's Law at low concentrations, thus receiving criticism for lacking of fundamental thermodynamic basis. The Freundlich isotherm is expressed by the equation below:

$$Q_e = a_F C_e^{b_F} \quad \text{Eq. (5)}$$

Eq. (5) can be rearranged to the linearized form:

$$\ln Q_e = \ln a_F + b_F \ln C_e \quad \text{Eq. (6)}$$

Where $a_F$ and $b_F$ are Freundlich constant in which $b_F$ is a measure of the surface heterogeneity.

Figure 5 shows the linear regression of Freundlich model and it was found to be well fit with experimental data with a $R^2$ value of 0.9843. $b_F$ value represented by the slope of the straight line was 2.2966 indicated a cooperative adsorption. Freundlich isotherm could be used for both physical and chemical adsorption also. This provided an insight that the $H_2S$ removal reaction was consisted both physical and chemical adsorption, in a cooperative way. In fact, oxidation of $H_2S$ into elemental sulfur could take part in the reactions, too.

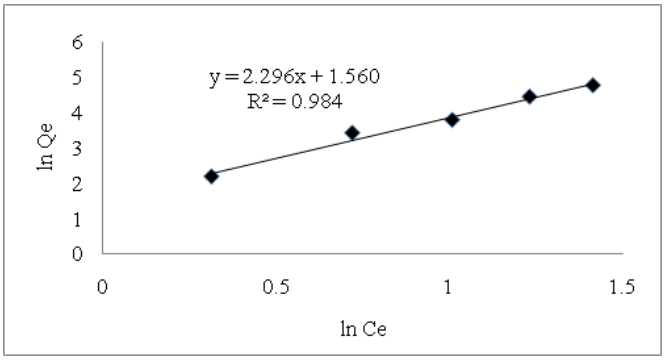


**Figure 5** Freundlich adsorption isotherm.

Dubinin-Radushkevich isotherm was extensively used for the adsorption using micro porous materials such as activated carbon.[27] It was derived based on the Polanyi potential theory of physical adsorption.[28] Similar with Freundlich isotherm, it received criticism for not being reduced to Henry's Law at low concentration. The Dubinin-Radushkevich isotherm is expressed in the equation below:

$$\ln Q_e = \ln Q_{DR} - k_{DR}\varepsilon^2 \quad \text{Eq. (7)}$$

Where $Q_{DR}$ is the maximum adsorption capacity; $k_{DR}$ is a constant related to the mean free energy of adsorption; ε is the Polanyi potential which can be calculated from the equation below:

$$\text{å} = RT \ln\left(1+1/C_e\right) \quad \text{Eq. (8)}$$

Combining Eqs. (7) and (8) would result Eq. (9)

$$Q_e = \ln Q_{DR} - R^2T^2k_{DR}\left(\ln\left(1+\frac{1}{C_e}\right)\right)^2 \quad \text{Eq. (9)}$$

where the constants could be obtained from the plot of lnQevs $\ln\left(\ln\left(1+\frac{1}{C_e}\right)\right)^2$ shown in Figure 6.

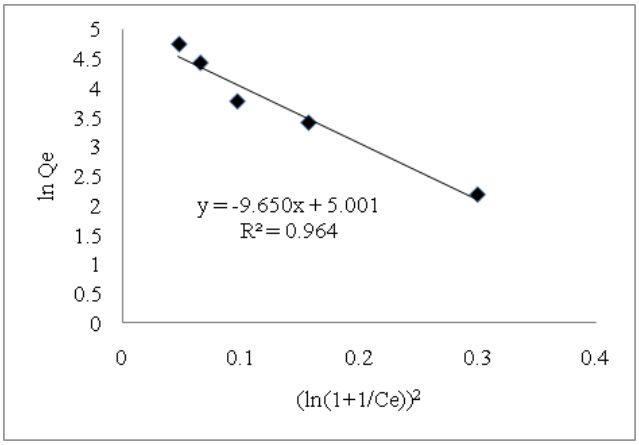


**Figure 6** Dubinin Radushkevich adsorption isotherm.

In addition, mean free energy of adsorption, E can be calculated from the $k_{DR}$ value using equation below:

$$E = \left(2k_{DR}\right)^{-0.5} \quad \text{Eq. (10)}$$

The Dubinin-Radushkevichisotherm was considered to be well fit with the experimental data with a $R^2$ value of 0.9642, while Freundlich isotherm was found to best fit with the experimental data. From the slope, $k_{DR}$ was calculated to be $1.5191 \times 10^{-6}$. From Eq. (10), the mean free energy of adsorption was calculated to be 573.7 J/mol.

Redlich-Peterson isotherm was derived by combining Langmuir and Freundlich isotherms in order to solve the argument of Freundlich isotherm that could not be reduced to Henry's Law at low concentration. The isotherm is expressed in the equation below:

$$Q_e = \frac{K_{RP}C_e}{1+a_{RP}C_e^{b_{RP}}} \quad \text{Eq. (11)}$$

Eq. (11) can be linearized as below:

$$\ln\left(K_{RP}\frac{C_e}{Q_e}-1\right)=b_{RP}\ln Ce+\ln a_{RP} \quad \text{Eq. (12)}$$

Where $K_{RP}$, $a_{RP}$ and $b_{RP}$ are Redlich-Peterson isotherm constants.

Eq. (12) contains three parameters so it is not possible to be solved using a linear regression method. However, a pseudo-linear form of the isotherm can be obtained by trial and error method to obtain $K_{RP}$ value with highest $R^2$ value. Figure 7 showed the optimum $K_{RP}$ value obtained via this method. Subsequently, the linear regression was performed and shown in Figure 8. The isotherm had a satisfactory fit with the experimental data because the $R^2$ value is 0.9633. From the slope and intercept, $a_{RP}$ and $b_{RP}$ were calculated as 0.1592 and -16.669, respectively.

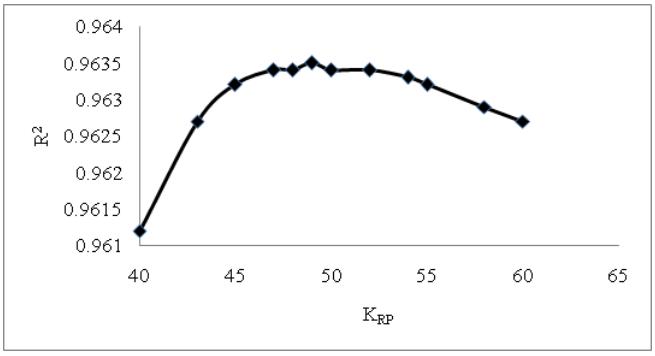


**Figure 7** $K_{RP}$ value for Redlich Peterson isotherm is 49, as determined from optimum $R^2$ value.

For comparison purpose, Table 2 shows the adsorption isotherm parameters obtained from other studies under different types of adsorbents and operating conditions. The isotherm parameter was not exactly identical, probably due to different type of adsorbents and operating conditions used.

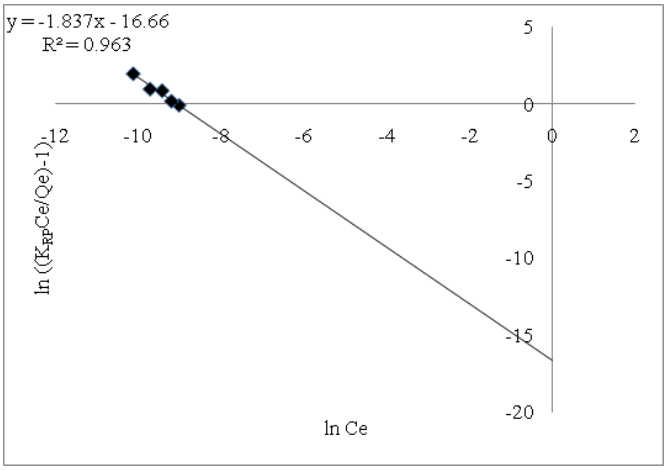


**Figure 8** Redlich Peterson adsorption isotherm.

### b. Adsorption kinetics

In the kinetic study, $H_2S$ adsorption was performed at different temperatures and the breakthrough curves of the reaction were shown in Figure 9. Pseudo-first order (Eq. 13) and pseudo-second order kinetic equation (Eq. 15) can be used to describe the kinetic of $H_2S$ adsorption. The breakthrough curve data was replotted using linearized pseudo-first order (Eq. 14) and pseudo-second order (Eq. 16) kinetic equation in order to investigate the kinetic parameters.

**Table 2** Isotherm parameters of other studies

| Adsorbent | Operating condition | Isotherm parameters | Reference |
|---|---|---|---|
| Organic packing material consisting pig manure and saw dust | 40-330 ppm $H_2S$, 23°C, residence time 8 s, flow rate 4 L/min, column size: 0.05m i.d. and 0.29m long. | Freundlich<br>KF=9.61<br>n=1.55 | 18 |
| Chemical activated palm shell activated carbon | 2000 ppm H2S, 25°C, flow rate 90mL/min, column size: 10.0 mm i.d. and 20 cm long. | Freundlich<br>KF=1.19 x 103<br>n=0.84 | 1 |
| $Na_2CO_3$ impregnated coal based activated carbon | 100-1000 ppm $H_2S$, 30°C, 1.5 g adsorbent, flow rate 120 mL/min, column size: 8mm in i.d., 200mm in length. | Langmuir<br>qm=9.4 mg/g<br>KL=0.018 m3/mg | 19 |
| Cerium oxide impregnated palm shell activated carbon | 1000-5000 ppm $H_2S$, 30°C, flow rate 500 mL/min, 0.1 g adsorbent. | Freundlich,<br>aF=2.2966<br>bF=1.5604<br>Dubinin-Radushevich<br>KDR=1.5191x10$^{-6}$ | This study |

$$\frac{dQ_t}{dt}=k_1\left(Q_e-Q_t\right) \quad \text{Eq. (13)}$$

Eq. (13) can be rearranged in linearized form as below:

$$\ln\left(Q_e-Q_t\right)=-k_1t+\ln Q_e \quad \text{Eq. (14)}$$

Where $Q_t$ and $k_1$ are the adsorption capacity at time t and pseudo-first order rate constant, respectively

$$\frac{dQ_t}{dt}=k_2(Q_e-Q_t)^2 \quad \text{Eq. (15)}$$

Eq. (15) can be rearranged in linearized form as below:

$$\frac{t}{Q_t}=\frac{1}{k_2Q_e^2}+\frac{t}{Q_e} \quad \text{Eq. (16)}$$

Where $k_2$ is the pseudo-second order rate constant.

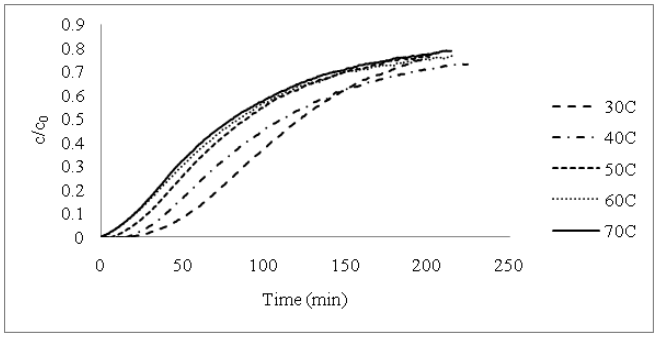


**Figure 9** Breakthrough curves of adsorption performed at different temperatures.

Pseudo-first order kinetic equation was found not to fit with the experimental data because the $R^2$ values were low, and therefore not reported. The parameters for pseudo-second order kinetic equation were calculated and tabulated in Table 3.

Subsequently, pseudo-second order rate constant, $_{K2}$ was used in the Arrhenius plot as shown in Figure 10. Arrhenius equation can be expressed in Eq. (17). The calculated activation energy for the $H_2S$ adsorption process was 11.7 kJ/mol.

$$k_2 = Ae^{-E_a/RT} \quad \text{Eq. (17)}$$

Eq. 17 can be rearranged in linearized form as below:

$$\text{in}k_2 = -\frac{E_a}{RT}\left(\frac{1}{T}\right) + \ln A \quad \text{Eq. (18)}$$

Where $E_a$ and A are the activation energy and pre-exponential factor, respectively.

**Table 3** Calculation for pseudo-second order kinetic equation

| S. no | Temperature °C | Slope | Intercept | $R^2$ | $Q_e$ | $K_2$ |
|---|---|---|---|---|---|---|
| 1 | 30 | 0.001023 | 0.438334 | 0.9282 | 977.526 | 2.39E-06 |
| 2 | 40 | 0.001112 | 0.453582 | 0.9514 | 899.1408 | 2.73E-06 |
| 3 | 50 | 0.00133 | 0.444889 | 0.9643 | 751.8114 | 3.98E-06 |
| 4 | 60 | 0.001276 | 0.447762 | 0.9619 | 783.6333 | 3.64E-06 |
| 5 | 70 | 0.001351 | 0.448577 | 0.9663 | 740.428 | 4.07E-06 |

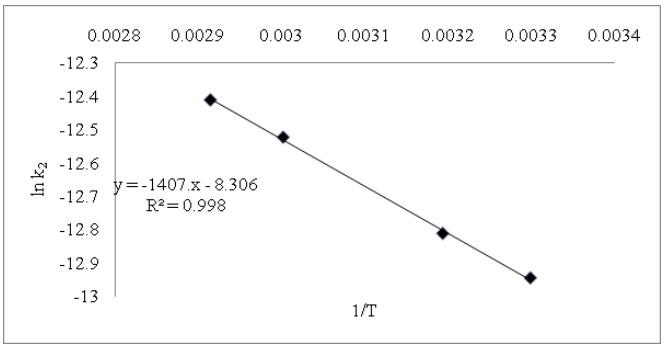


**Figure 10** Arrhenius plot from pseudo-second order kinetic constant.

### c. Adsorption thermodynamic

For the thermodynamic study, Van't Hoff's equation as expressed in Eq. (19) can be used to determine the enthalpy change (ΔH) and entropy change (ΔS).

$$\ln\frac{Q_e}{C_e} = -\frac{\Delta H}{RT} + \frac{\Delta S}{R} \quad \text{Eq. (19)}$$

Eq. (19) was plotted using the experimental data and high correlation coefficient of 0.9990 was obtained. From the slope and intercept, enthalpy change (ΔH) and entropy change (ΔS) were calculatedto be -6.0 kJ/mol and 25.7 J/mol.K, respectively. Negative enthalpy change value indicated the reaction was exothermic and the adsorption capacity would reduce with the increasing temperature. Positive entropy change on the other hand, denoted a more ordered orientation of $H_2S$ molecules as adsorb ate than free molecules in the bulk stream.

Gibbs free energy change for the adsorption process was calculated using Eq. (20) below:

$$\Delta G = \Delta H - T\Delta S \quad \text{Eq. (20)}$$

The calculated Gibbs free energies for the adsorption temperature range (30-70˚C) were between -1.77 and -2.80 kJ/mol. The negative Gibbs free energy value indicated that the adsorption reaction is a spontaneous reaction. From the values of these Gibbs free energy, enthalpy change and entropy change, it can be concluded that the sorption process was driven by both enthalpy and entropy.[6] Process driven by enthalpy denotes that the system achieves a more stable state by releasing heat energy. On the other hand, entropy driven process denotes the system proceeds in the way that more randomness or chaos occur in the arrangement of molecules. The indication for selection is the comparison between the absolute values of Δ Hand TΔS.

### d. Breakthrough curve models

Relationship between breakthrough time and bed height was modified from the Bed Depth Service Time (BDST) model to result following equation:

$$t_b = \frac{q_b}{c_o F}Z - \frac{1}{K_a c_o}\ln\left(\frac{c_o}{c_b} - 1\right) \quad \text{Eq. (21)}$$

Whereas $t_b$ is the breakthrough time, $q_b$ is the breakthrough sorption capacity, $c_o$ is the initial $H_2S$ concentration, F is the volumetric flow rate, Z is the bed height, $K_a$ is the rate constant in BDST model, $c_b$ is the $H_2S$ concentration at breakthrough.

Eq. (21) can be represented in the simpler form,

$$t_b = mZ - C \quad \text{Eq. (22)}$$

Whereas m describes the time required for the sorption zone to travel a unit length through the sorbent, and C is the intercept of the curve on axis-y which can be used to calculate the rate constant, $K_a$.

Figure 11 shows the BDST model for the $H_2S$ removal process. The high $R^2$ value shows a good linear relationship between breakthrough time and bed depth. This denotes a good chance for the extrapolation of bed height to obtain column service time in the scale up operation. The slope represents the sorption zone travels at the speed of 4395.7 min/m across the column and the rate constant $K_a$ is calculated to be 0.0231 L/mg.min.

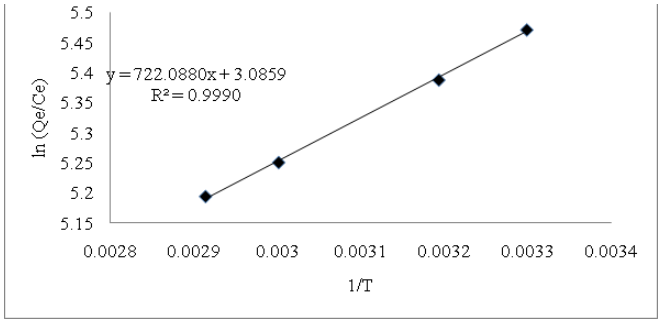


**Figure 11** Van't Hoff plot.

In the design of a column sorption process, the breakthrough curve prediction is necessary. Mathematical models can be used to describe these packed bed sorption processes. However, most of developed models often require additional experimentation and non-linear curve fitting in order to determine preliminary parameters such as isotherm and mass transfer parameters. In addition, complex analytical solutions for differential equations in the models are not available. This resulted difficulties and inconvenience therefore impractical to serve the original purpose.[20] Thus, empirical models have been developed in order to describe the dynamic behavior of the sorption column in relatively easier ways such as Bohard-Adams (BA), Wolborska, Thomas, Yoon-Nelson (YN) and Belter. The Belter model modified by Chu was also discussed in this study.[1] The mathematical models are shown in equations below:

Bohart-Adams: $$\ln \frac{c}{c_o} = k_{BA} cot - k_{BA} q_{BA} \frac{Z}{v} \quad \text{Eq. (23)}$$

Wolborska: $$\ln \frac{c}{c_o} = \frac{\beta_a c_o}{q_w} t - \frac{\beta_a Z}{v} \quad \text{Eq. (24)}$$

Thomas: $$\ln\left(\frac{c_o}{c} - 1\right) = \frac{k_{Th} q_{Th} m}{F} - \frac{k_{Th} c_o}{F} V \quad \text{Eq. (25)}$$

Yoon-Nelson: $$\ln\left(\frac{c}{c_o - c}\right) = k_{YN}(t - \tau) \quad \text{Eq. (26)}$$

Belter: $$\frac{c}{c_o} = \frac{1}{2}\left(1 + \text{erf}\left[\frac{t-\tau}{\sqrt{2}\sigma\tau}\right]\right) \quad \text{Eq. (27)}$$

$\text{Chu}_1$: $$\frac{c}{c_o} = \frac{1}{2}\left(1 + \text{erf}\left[\frac{(t-\tau)\exp(\sigma t/\tau)}{\sqrt{2}\sigma\tau}\right]\right) \quad \text{Eq. (28)}$$

$\text{Chu}_2$: $$\frac{c}{c_o} = \frac{1}{2}\left(1 + \text{erf}\left[\frac{(t-\tau)\exp(-\sigma t/\tau)}{\sqrt{2}\sigma\tau}\right]\right) \quad \text{Eq. (29)}$$

where as $c_o$ is initial $H_2S$ concentration, c is $H_2S$ concentration at time t, $k_{BA}$, $k_{Th}$ and $k_{YN}$ are rate constants, $q_{BA}$, $q_w$ and $q_{Th}$ are sorption capacities, Z is height of the sorbent bed, v is linear velocity, $\beta_a$ is kinetic coefficient of external mass transfer, F is the volumetric flow rate, m is amount of sorbent, V is the treated biogas volume, τ is time when $c/c_o = 0.5$, σ is standard deviation of the slope of the breakthrough curve, and erf(t) is the error function of t.

Linear dependences of Bohart-Adams and Wolborska models are the same and therefore same plot can be used for the calculation of model parameters. In addition, Yoon-Nelson and Thomas models also share some similarities with each other that could result same correlation coefficient, $R^2$ value because V, volume of treated biogas is actually corresponding to the elapsed time, t. Thus, both Bohart-Adams and Wolborska; Yoon-Nelson and Thomas models are placed together in the plot, respectively. Belter model and Chu modifications have different calculation method for $R^2$ values. They contain two model parameters, σ and τ that were empirical estimated in order to obtain the best fit of experimental data.

The experimental data was compared with the model and $R^2$ value was calculated based on the equation below:

$$R^2 = 1 - \frac{SS_{res}}{SS_{tot}} \quad \text{Eq. (30)}$$

$$SS_{res} = \sum_{i=1}^{n}\left(x_i - \hat{x}_i\right)^2 \quad \text{Eq. (31)}$$

$$SS_{tot} = \sum_{i=1}^{n}\left(x_i - \bar{x}_i\right)^2 \quad \text{Eq. (32)}$$

Whereas $SS_{res}$ is residual sum of squares, $SS_{tot}$ is total sum of squares, n is the number of experimental data, $x_i$ is experimental data, $\overline{X}_i$ is calculated data, $\overline{X}_i$ is mean of experimental data.

Figure 12 showed all the $R^2$ values of all models for conducted experiments. From the distribution of $R^2$ values, it was noticeable that model $\text{Chu}_2$ has the highest $R^2$ value among all the models. Additionally, Belter model also gave substantially high $R^2$ value to indicate a good fit of the experimental data. Surprisingly, no Bohart-Adams, Wolborska, Yoon-Nelson and Thomas models were found able to fit the experimental well. In fact,[19] also reported $R^2$ value lower than 0.80 when they used linearized Thomas model to fit their experimental data. When non-linear regression method was used, higher $R^2$ in the range of 0.80-0.90 were obtained but still cannot be considered as well fitting with the experimental data.

The Belter model and those modified by Chu[1] do not include diffusional coefficients in their model. Instead, error function (erf) is used to describe the breakthrough curve. These equations are only valid for the case that the system is favorable sorption type, which evidenced by the S shape breakthrough curve. For unfavorable sorption type, addition of diffusional coefficients to the models is necessary. Belter model is capable to predict the symmetric breakthrough curve. However, the $H_2S$ removal breakthrough curve was found to be

asymmetric and therefore the $R^2$ values for Belter model show slightly less than 1.0. On the other hand, Belter model was modified by Chu [1] in order to fit the experimental data regardless the breakthrough curve is symmetry or asymmetry. Therefore in this study, $Chu_2$ model has shown excellent fit with experimental data.

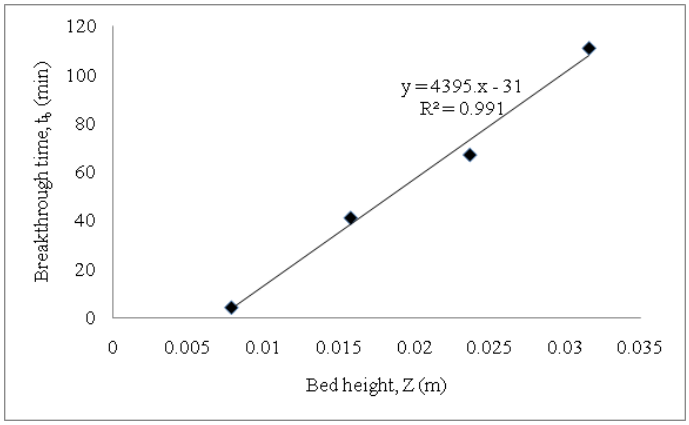


**Figure 12** BDST model.

Belter model contains two adjustable parameters.[1]Modified the Belter model by adding an exponential term and did not introduce any new adjustable parameters. After modifications, the model became a fast and accurate way to describe the breakthrough curve, comparing to conventional mass balance based model which require complex mathematical calculation. Chu model only requires breakthrough data calibration in order to find the suitable value for the two adjustable parameters. Significant improvement was shown in this study as comparing $R^2$ values for Belter and $Chu_2$ models as shown in Figure 13, Figure 14 shows the linear relationship between $t_o$ and $1/v$ ($v$ is superficial velocity). The linearity indicated that the $t_o$ value could be estimated to predict the breakthrough curve of $H_2S$ removal process using other superficial velocity. However, one should note that the major drawback of this model is the correlation was calibrated using the available experimental data only, in which details of the process characteristics were not known. In addition, the values of $t_o$ and σ could vary with different process parameters. Therefore, extrapolation could be inadequate and inaccurate unless effects of major process parameters on the values of $t_o$ and σ are investigated.

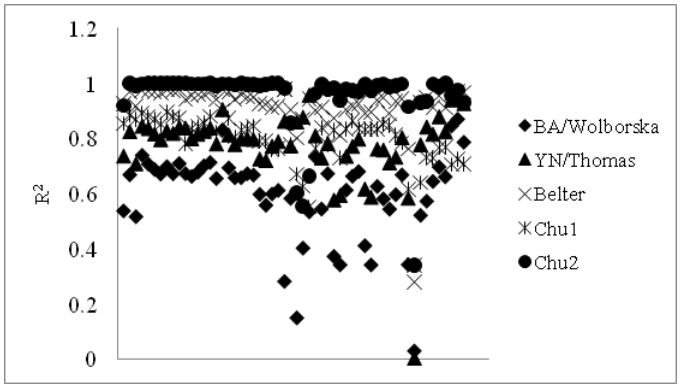


**Figure 13** $R^2$ value for various breakthrough models.

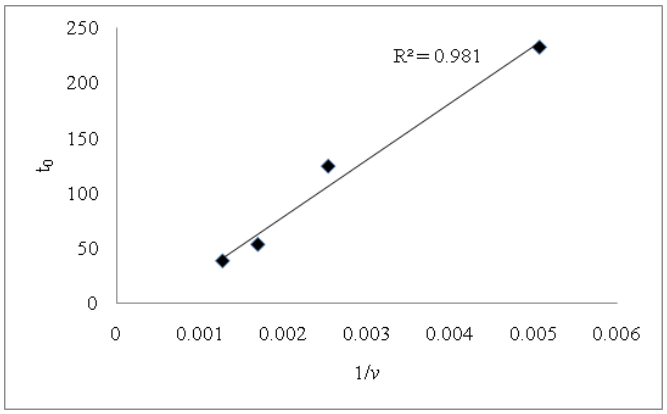


**Figure 14** Linear relationship between $t_0$ and $1/v$.

## Conclusion

Dynamic adsorption was successfully applied in the calculation for adsorption isotherm, kinetics, thermodynamics and breakthrough curve modeling. Data analysis showed that Freundlich sorption isotherm can best described the sorption behavior. The isotherm parameter was not identical with other studies because different type of adsorbents and operating conditions were used. Thermodynamic study showed that enthalpy change (ΔH) and entropy change (ΔS) were calculated to be -6.0 kJ/mol and 25.7 J/mol.K. The sorption was pseudo-second order with activation energy 11.7 kJ/mol and rate constant was between 2.387-4.066 X $10^{-6}$ g/mg.min for 30-70˚C. Breakthrough curve was fitted best by using breakthrough model developed by.[1]

## Acknowledgments

The authors would like to acknowledge the financial supports from UniversitiTunku Abdul Rahman UTARRF (Grant No. IPSR/RMC/UTARRF/2015-C2/L03), My Brain 15 Program, Knowledge Transfer Program (Grant No. 203/PJKIMIA/6750045), FELDA Palm Industries SdnBhd, and Universiti Sains Malaysia RU-PRGS (Grant No. 1001/PJKIMIA/8045042).

## Conflict of interest

The author declares no conflict of interest.

## References

1. Chu KH. Improved fixed bed models for metal biosorption. *Chemical Engineering Journal*. 2004;97(2–3):233–239.
2. Shukla NB, Madras G. Kinetics of adsorption of methylene blue and rhodamine 6G on acrylic acid–based superadsorbents. *Journal of Applied Polymer Science*. 2012;126(2):463–472.
3. Zawani Z, Chuah LA, Choong TSY. Equilibrium, kinetics and thermodynamic studies: adsorption of Remazol Black 5 on the palm kernel shell activated carbon (PKS–AC). *European Journal of Scientific Research*. 2009;37(1):67–76.
4. JiaGuo, Ye Luo, Aik Chong Lua, et al. Adsorption of hydrogen sulphide ($H_2S$) by activated carbons derived from oil–palm shell. *Carbon*. 2007;45(2):330–336.

5. Piar Chand, Arun Kumar Shil, Mohit Sharma, et al. Improved adsorption of cadmium ions from aqueous solution using chemically modified apple pomace:Mechanism, kinetics and thermodynamics. *International Biodeterioration & Biodegradation*. 2014;90:8–16.
6. Shuang Yang, Lingyun Li, Zhiguo Pei, et al. Adsorption kinetics, isotherms and thermodynamics of Cr(III) ongraphene oxide. Colloids and Surfaces A: Physicochem. Eng. Aspects. 2014;457(5):100–106.
7. HongxuGuo, Jianhua Chen, Wen Weng, et al. Adsorption behavior of Congo red from aqueous solution on$La_2O_3$–doped $TiO_2$ nanotubes. *Journal of Industrial and Engineering Chemistry*. 2014;20(5):3081–3088.
8. Jinbei Yang, Meiqiong Yu, Ting Qiu. Adsorption thermodynamics and kinetics of Cr(VI) on KIP210 resin. *Journal of Industrial and Engineering Chemistry*. 2014;20(2):480–486.
9. Xuan Zhou, Honghong Yi, Xiaolong Tang, et al. Thermodynamics for the adsorption of $SO_2$, NO and $CO_2$ from flue gason activated carbon fiber. *Chemical Engineering Journal*. 2012;200–202:399–404.
10. Llorens J, Pera Titus M. A thermodynamic analysis of gas adsorption on micro porous materials: evaluation of energy heterogeneity. *Journal of Colloid and Interface Science*. 2009;331(2):302–311.
11. Yi Peng Teoh, Moonis Ali Khan, Thomas SY Choong. Kinetic and isotherm studies for lead adsorption from aqueous phase on carbon coated monolith. *Chemical Engineering Journal*. 2013;217:248–255.
12. Xue Song Wang, Li Fang Chen, Fei Yan Li, et al. Removal of Cr (VI) with wheat–residue derived black carbon:Reaction mechanism and adsorption performance. *Journal of Hazardous Materials*. 2010;175(1–3):816–822.
13. Ahmad B Albadarin, Jiabin Mo, Yoann Glocheux, et al. Preliminary investigation of mixed adsorbents for the removal of copper and methylene blue from aqueous solutions. *Chemical Engineering Journal*. 2014;255:525–534.
14. Yuh Shan Ho . Pseudo–Isotherms Using a Second Order Kinetic Expression Constant. *Adsorption*. 2004;10(2):151–158.
15. Mamdoh R Mahmoud, Gehan E Sharaf El deen, Mohamed A Soliman. Surfactant–impregnated activated carbon for enhanced adsorptive removal of Ce(IV) radionuclides from aqueous solutions. *Annals of Nuclear Energy*. 2014;72:134–144.
16. Adriana P Vieira, Sirlane AA Santana, Cícero WB Bezerra, et al. Removal of textile dyes from aqueous solution by babassu coconut epicarp (*Orbignyaspeciosa*). *Chemical Engineering Journal*. 2011;173(2):334–340.
17. Johnny Saavedra, Camilah Powell, BasuPanthi, et al. CO oxidation over $Au/TiO_2$ catalyst:Pretreatment effects, catalyst deactivation, and carbonates production. *Journal of Catalysis*. 2013;307:37–47.
18. Lu C, Su F, Hsu SC, et al. Thermodynamics and regeneration of $CO_2$ adsorption on mesoporous spherical–silica particles. *Fuel Processing Technology*. 2009;90(12):1543–1549.
19. Yan G, Viraraghavan T. Heavy metal removal in a biosorption column by immobilized M rouxii biomass. *Bioresource Technology*. 2001;78(3):243–249.
20. Trgo M, Medvidovic Nv, Peric J. Application of mathematical empirical models to dynamic removal of lead on natural zeolite clinoptilolite in a fixed bed column. *Indian Journal of Chemical Technology*. 2011;18(2):123–131.
21. Wang S, Peng Y. Natural zeolites as effective adsorbents in water and wastewater treatment. *Chemical Engineering Journal*. 2010;156(1):11–24.
22. Handoaui O. Dynamic sorption of methylene blue by cedar sawdust and crushed brick in fixed bed columns. *Journal of Hazardous Materials*. 2006;138(2):293–303.
23. Sag Y, Aktay Y. Application of equilibrium and mass transfer models to dynamic removal of Cr(VI) by chitin in packed column reactor. *Process Biochemistry*. 2001;36(12):1187–1197.
24. Ghorai S, Pant KK. Investigations on the column performance of fluoride adsorption by activated alumina in a fixed bed. *Chemical Engineering Journal*. 2004;98(1–2):165–173.
25. C Nguyen, DD Do. The Dubinin–Radushkevich equation and the underlying microscopic adsorption description. *Carbon*. 2001;39(9):1327–1336.
26. GO Wood. Affinity coefficients of the Polanyi/Dubinin adsorption isotherm equations:A review with compilations and correlations. *Carbon*. 2001;39(3):343–356.
27. Ying Chu Chen, Chungsying Lu. Kinetics, thermodynamics and regeneration of molybdenum adsorption in aqueous solutions with NaOCl–oxidized multiwalled carbon nanotubes. *Journal of Industrial and Engineering Chemistry*. 2014;20(4):2521–2527.
28. A Barona, A Elias, A Amurrio, et al. Hydrogen sulphide adsorption on a waste material used in bioreactors. *Biochemical Engineering Journal*. 2005;24(1):79–86.
29. Yonghou Xiao, Shudong Wang, Diyong Wu, et al. Experimental and simulation study of hydrogen sulfide adsorption on impregnated activated carbon under anaerobic conditions. *Journal of Hazardous Materials*. 2008;153(3):1193–1200.